L-487

ARR No. 3D17

NATIONAL ADVISORY COMMITTEE FOR AERONAUTICS

WARTIME REPORT

ORIGINALLY ISSUED
April 1943 as
Advance Restricted Report 3D17

FREE-FLIGHT-TUNNEL INVESTIGATION OF THE EFFECT OF THE FUSELAGE LENGTH AND THE ASPECT RATIO AND SIZE OF THE VERTICAL TAIL ON LATERAL STABILITY AND CONTROL

By Joseph A. Shortal and John W. Draper

Langley Memorial Aeronautical Laboratory
Langley Field, Va.

NACA

WASHINGTON

NATIONAL ADVISORY COMMITTEE FOR AERONAUTICS

ADVANCE RESTRICTED REPORT

FREE-FLIGHT-TUNNEL INVESTIGATION OF THE EFFECT OF THE FUSELAGE LENGTH AND THE ASPECT RATIO AND SIZE OF THE VERTICAL TAIL ON LATERAL STABILITY AND CONTROL

By Joseph A. Shortal and John W. Draper

SUMMARY

Tests have been made in the NACA free-flight tunnel to determine the effect of the fuselage length and the aspect ratio and size of the vertical tail on lateral stability and control. Fuselages of two different lengths and various vertical tail surfaces were used on a powered model in the investigation. Both flight and force tests were made.

The tests indicated that a deficiency of tail area could not be overcome by an increase in fuselage length because the unstable moment of the fuselage as well as the tail effectiveness increased directly with the tail length. With a positive degree of directional stability, however, an increase in tail length provided increased stability. An increase in the aspect ratio of the vertical tail from 1.00 to 2.28 increased the tail effectiveness by 67 percent. Power had a stabilizing effect on directional stability for single vertical tails; whereas a destabilizing effect was observed for twin tails. Dorsal fins improved the directional stability at large angles of yaw.

INTRODUCTION

The demand for increased performance of pursuit airplanes has made it imperative that the tail surfaces be restricted to the minimum areas required for satisfactory directional stability and control. One possible means of compensating for a reduction in tail size is to lengthen

the fuselage. In order to provide data on the possible reductions in tail area with an increased tail length, tests have been made in the NACA free-flight tunnel of fuselages of two different lengths on a 1/10-scale, dynamic, powered model of a typical pursuit airplane. The long fuselage incorporated some additional drag-reducing features: The engine cowling was enlarged to accommodate the auxiliary cooling ducts and the mean line of the fuselage was modified. The nose of the fuselage was extended somewhat to maintain the original location of the center of gravity.

In the investigation, the lateral-stability and lateral-control characteristics of the model in flight in the tunnel were determined with both fuselage lengths for four single vertical tails with two different areas and two aspect ratios. Dorsal fins were added to two of the tails. The flight tests were supplemented by force tests on the six-component balance in the same tunnel. In addition, force tests were made with a twin tail having the same total area and the same aspect ratio as the largest single tail.

SYMBOLS AND COEFFICIENTS

C_L lift coefficient (L/qS)

C_D drag coefficient (D/qS)

C_l rolling-moment coefficient (L/qbS)

C_m pitching-moment coefficient $(M/q\bar{c}S)$

C_Y lateral-force coefficient (Y/qS)

C_n yawing-moment coefficient (N/qbS)

where

L lift; rolling moment

D drag

M pitching moment

Y lateral force

N yawing moment

and

q	dynamic pressure $(\frac{1}{2}\rho V^2)$
q_t	dynamic pressure at tail location
ρ	density of air, slug per cubic foot
V	airspeed, feet per second
S	model wing area, square feet
S_t	vertical tail area, square feet
b	model wing span, feet
$\bar{c}$	average model wing chord, feet
T_c	thrust disk-loading coefficient $(T/\rho V^2 D^2)$
T	thrust, pounds
D	diameter of model propeller, feet
Q	torque, pound-foot
Q_c	torque coefficient $(Q/\rho V^2 D^3)$
α_T	angle of attack of thrust line, degrees
δ_f	flap deflection, degrees
ψ	angle of yaw of model, degrees
m	slope of lift curve per radian
l	tail length from center of gravity to rudder hinge line, feet
A	aspect ratio
η_t	tail efficiency factor
C_{n_β}	rate of change of yawing-moment coefficient with angle of sideslip in radians $(dC_n/d\beta)$
β	angle of sideslip, degrees

All forces and moments are given with respect to the stability axes.

APPARATUS

Wind Tunnel

The details and the operation of the NACA free-flight tunnel are described in reference 1. Dynamic models may be flown in the tunnel under the remote control of a pilot seated below the test section. The pilot observes the stability and control characteristics of the model while attempting to fly it along a fixed course. The pilot's observations are supplemented by motion-picture records of the model in flight. A photograph of the model as tested in flight is shown in figure 1.

Balance

The six-component balance is located on top of the tunnel test section as shown in figure 2. A removable strut is used to attach the model to the balance.

A diagrammatic sketch of the balance proper is presented as figure 3. The linkage of the balance is arranged to give the moments directly with respect to a point located within the model. The angles of attack and yaw may be varied during the operation of the balance. The entire balance rotates with the model in yaw making the balance axes coincide with the stability axes of the model.

Details of a typical balance-beam installation are shown in figure 4. Three types of knife edge are used: emery, block, and music wire. The forces are manually balanced with unit weights and a sliding rider. Contact points at the end of the beam indicate an out-of-balance condition by lighting neon lamps in the circuit.

A photograph of the model mounted on the balance strut is given as figure 5.

Model

The model used in the investigation was a 1/10-scale dynamic model of the Republic XP-41 airplane. A three-

view drawing of the model showing how the original fuselage was modified to form the long fuselage is given as figure 6. The model was constructed chiefly of balsa with spruce reinforcements. The fuselage was hollow and contained the control-operating mechanisms and a 3/4-horsepower electric motor connected directly to a 13-inch propeller.

Three-quarter-front and side views of the model with the normal fuselage are given as figure 7; with the long fuselage, as figure 8.

The mass and dimensional characteristics of the airplane represented by the 1/10-scale model are given in the following table:

Weight, pounds	6770
Moments of inertia, slug-feet^2	
I_X	3390
I_Y	5309
I_Z	7953
Span, feet	36
Wing area, square feet	223.7
Wing loading, pounds per square foot	30.3
Aspect ratio	5.8
M.A.C., inches	74.6
Horizontal tail area, square feet	54.0
Brake horsepower	1750

The horizontal tail on the model was 30 percent larger than the horizontal tail specified for the original airplane. The various vertical tails used in the investigation are shown in figures 9 to 11. The dimensional characteristics of these tails and the tail lengths used, measured from the center of gravity to the rudder hingeline, are included in table 1.

TESTS AND RESULTS

Test Conditions

All the tests were made with the center of gravity at 26.4 percent of the mean aerodynamic chord. The landing gear was extended for all tests.

Flight Tests

In the flight tests the elevator-trim setting was varied over a range sufficient to cover the airspeed range of the model. Although the stability and control characteristics of the model were noted at each airspeed, particular attention was given the low-speed conditions. The following procedure was followed and ratings for each condition were assigned by the pilot:

(a) The general stability characteristics were determined by noting the behavior of the model with controls fixed

(b) The control requirements were noted when the ailerons and rudder were used together for lateral control

(c) The behavior of the model was noted when the ailerons alone were used for lateral control

(d) Finally, the rudder was used as the sole means of lateral control and its effectiveness in picking up a low wing was noted.

The ratings given by the pilot for the various flight tests are given in table II. A rating of "A" is considered necessary with ailerons and rudder used together, a rating of "B" is considered satisfactory for ailerons alone, and a rating of "C" is considered satisfactory for flights with rudder used alone for lateral control.

Force Tests

In the force tests, the dynamic pressure was held constant at 2.825 pounds per square foot. The speed of the model propeller was varied to represent thrust coefficients from -0.03 to 0.51. A thrust coefficient of 0.51 represents 1750 brake horsepower with a propeller efficiency of 80 percent at an airspeed of 118 miles per hour. The torque coefficient associated with the thrust coefficient of 0.51 represented a full-scale propeller speed of 1860 rpm. Most of the tests were made with flaps retracted because the flight tests indicated that this condition was the most critical for directional stability.

The results of the force tests are given in figures 12 to 21. The basic aerodynamic characteristics of the model

with each fuselage without propellers are given in figure 12. The lateral-stability characteristics of the model with each fuselage and with vertical tail off are given in figure 13. The effect of flaps on the lateral-stability characteristics of the model with normal fuselage, tail 1, and windmilling propeller is shown in figure 14. The directional-stability characteristics of the model with the normal fuselage and various vertical tails are given in figure 15 for propeller windmilling and in figure 16 for power on. Similar data are given in figures 17 and 18 for the model with the long fuselage. A cross plot of C_{n_β} against the ratio of tail length to wing span is given in figure 19. In figure 20, the increment of yawing-moment coefficient due to vertical tails of two different aspect ratios are given for the model with long fuselage and propeller windmilling. The variation of the rolling- and yawing-moment and lateral-force coefficients with thrust and torque coefficient are given for the model with the long fuselage for various vertical-tail configurations in figure 21.

The values of the directional-stability derivative C_{n_β} for all conditions tested are summarized in table I. The increment of directional stability contributed by the vertical tails $\Delta C_{n_{\beta_t}}$ was obtained by deducting the slope with the tail removed from the slope with the tail on. The calculated values of $\Delta C_{n_{\beta_t}}$ given in table I were obtained by the equation

$$\Delta C_{n_{\beta_t}} = \frac{S_t}{S} \frac{l}{b} m \frac{q_t}{q}$$

The ratio q_t/q was assumed to be unity with a windmilling propeller for the single tails and for both power conditions for the twin tails. For the power-on conditions with single tails, a ratio of $\frac{q_t}{q} = 1 + \frac{8T_c}{\pi}$ was used. The ratio of the measured increments to the calculated values of $\Delta C_{n_{\beta_t}}$ gives an indication of the tail efficiency of each arrangement.

DISCUSSION

Effect of Fuselage Length

The direct effects of fuselage length on the lateral-stability characteristics of the model as determined from the force tests with the vertical tail removed are shown in figure 13. The effects of tail length on the directional-stability derivative C_{n_β} for different tail and power conditions are shown in figure 19. The long fuselage had a considerably greater unstable yawing moment that the normal fuselage without vertical tail surfaces. The increase was approximately proportional to the increase in fuselage length. Part of this increase in unstable moment with the long fuselage was undoubtedly due to the larger cowling and the more forward position of the propeller on the long fuselage but the greatest effect was believed to be due to the increased length. With power on, the unstable moment increased with both fuselages but the increase was more pronounced with the long fuselage.

With vertical tail 2, which has low aspect ratio, practically neutral directional stability was obtained with either fuselage. This effect indicated that the increased moment arm of the long fuselage provided only sufficient additional yawing moment to offset the additional unstable moment of the fuselage. The increased tail length provided the expected increase in the increment of directional stability contributed by the tail as indicated by the fact that the tail-efficiency factors η_t in table I had approximately the same values.

With tail 3 or 4, which has higher aspect ratio than tail 2, somewhat higher values of C_{n_β} were obtained with the long fuselage than with the normal one for either power on or power off. This effect is particularly significant for it means that, although a deficiency in C_{n_β} cannot be overcome by increasing the tail length, increasing the tail length of an airplane that has a positive degree of directional stability will allow some reduction in tail area. This effect is to be expected inasmuch as both the unstable moment of the fuselage and the increment of moment from the tail are directly proportional to the fuselage length.

The flight-test results were in good agreement with the results of the force tests. The same tail area was required with the long fuselage as with the normal one when either tail 1 or 2, which has low aspect ratio, was used. Although tail 2 on the long fuselage provided the same tail volume as tail 1 on the normal fuselage, the flight tests indicated somewhat less stability than when tail 1 was used. In fact, with tail 2, the model with the long fuselage would trim at an angle of yaw of either 10° or -10°, verifying the flat spot in the yawing-moment curve of figure 17. With either tail 3 or 4, which has higher aspect ratio than tail 1 or 2, however, good flights were obtained with either fuselage as indicated in table II. Tail 4 on the long fuselage provided the same tail volume as tail 3 on the normal fuselage. Tail 3 on the long fuselage provided the best flying arrangement for the model.

Effect of Vertical-Tail Shape

A study of the yawing-moment curves of figures 15 and 17 indicated that the flat spot near zero yaw was chiefly a result of insufficient tail moment although there was undoubtedly some shielding of the vertical tail at angles of yaw from -10° to 10°. This effect is shown in figure 20 in which the increments of yawing-moment coefficient due to the vertical tail are plotted for tails 1 and 3 on the long fuselage. With either tail, the slope is constant for angles of yaw from 10° to -10°.

The first change in tail shape, designed to provide more tail moment, was simply an increase in the aspect ratio of the original tails without change of area. Tails 3 and 4 have the same area as tails 1 and 2 but have aspect ratios of 2.28 instead of 1.00. With either tail 3 or 4, the flat spot in the yawing-moment curves was eliminated for the windmilling condition as shown in figures 15 and 17. The increments in yawing-moment slope due to the tails $\Delta C_{n_{\beta_t}}$ given in table I indicate that the tails which have the higher aspect ratio provided approximately the increase in slope that would be expected. The effectiveness of the vertical tail was increased 67 percent by this increase of aspect ratio.

Either tail 3 or 4 provided more satisfactory flying characteristics and appeared to be more effective in every respect than tail 1 or 2. From a simple analysis the con-

dition of neutral stability encountered with tails 1 and 2 in the windmilling condition at small angles of yaw might be expected to provide a steadier flying airplane inasmuch as simple side gusts would not change the heading of the airplane. In the flight tests of the model in the tunnel, however, the steadiest flights were obtained with the vertical tails that provided a positive degree of directional stability through zero yaw, particularly with tail 3. With tail 1 or 2, the model would not hold any particular heading but would wander from 5° left yaw to 5° right yaw. The low dihedral of the model prevented any objectionable rolling with the changes in angle of yaw and the model could be flown continuously. The wandering condition, however, was objectionable and was not improved by lengthening the fuselage. With tail 3, however, satisfactory and steady flights were obtained and the model was not unduly disturbed by the turbulent air stream of the tunnel.

Another attempt was made to eliminate the flat spot on the yaw curves by dividing the original tail into twin tails and locating them near the stabilizer tips on the upper surface to get the tail area away from the influence of the fuselage. The aspect ratio and the total area of the twin tails (tail 5) were the same as for tail 3. A good yawing-moment curve was obtained with these tails with a windmilling propeller (fig. 17) but, with power on (fig. 18), a flat spot was noticed at negative angles of yaw. Inasmuch as tails 3 and 4 were satisfactory, no further tests were made with the twin tails.

With the propeller windmilling, the twin tails, tail 5, provided more tail moment than tail 3 apparently because they were located away from the reduced velocity region near the fuselage. With power on, however, tail 5 was missed by the slipstream at low angles of yaw and the increased unstable moment of the fuselage with power on reduced the over-all stability of the model as indicated in figure 19.

The dorsal fins shown in figure 10 with tail 1 and in figure 11 with tail 3 were principally effective in providing directional stability at large angles of yaw. Only a slight effect was measured at small angles of yaw. The stability characteristics of the model in flight were not changed in the normal-flight range by the addition of dorsal fins. It is believed, however, that the dorsal fins would restrict the trim angles of yaw to reasonable values for the high-power conditions.

Effect of Power

The increase in the unstable yawing moment of the fuselage due to power shown in figure 13 was more pronounced with the long fuselage than with the normal one. The increase is apparently due to the increased velocity of the slipstream passing over the unstable fuselage. Power also introduced a lateral force, a rolling moment, and a yawing moment at zero yaw that were approximately proportional to the torque coefficient as shown in figure 21.

The increase in directional stability $\Delta C_{n_{\beta_t}}$ contributed by the various single tails with power on was a direct function of the slipstream velocity. This effect is indicated by the fact that the efficiency factors η_t were substantially the same with power on as they were with a windmilling propellor when an average slipstream-velocity factor was used in the calculations.

In flight the model was more stable with power on for all conditions tested. The tendency for the model to wander in yaw with tail 1 or 2 was eliminated when power was applied.

CONCLUSIONS

From the results of free-flight-tunnel tests of a 1/10-scale dynamic model, on which two fuselage lengths and various vertical-tail arrangements were used, the following conclusions were drawn:

1. Increasing the length of the fuselage was not a satisfactory means of converting a neutrally stable airplane into a directionally stable one because the unstable moment of the fuselage as well as the tail effectiveness increased directly as the fuselage length.

2. Increasing the length of the fuselage of a directionally stable airplane allowed some reduction in vertical tail area.

3. The use of vertical tail surfaces of high aspect ratio was definitely beneficial. Increasing the aspect ratio from 1.00 to 2.28 increased the tail effectiveness by 67 percent.

4. Power had a stabilizing effect on directional stability for single tails and a destabilizing effect for twin tails.

5. Dorsal fins improved the directional stability at large angles of yaw.

Langley Memorial Aeronautical Laboratory,
National Advisory Committee for Aeronautics,
Langley Field, Va.

REFERENCES

1. Shortal, Joseph A., and Osterhout, Clayton J.: Preliminary Stability and Control Tests in the NACA Free-Flight Wind Tunnel and Correlation with Full-Scale Flight Tests. T.N. No. 810, NACA, 1941.

TABLE I

ANALYSIS OF DIRECTIONAL STABILITY DERIVATIVE C_{n_β}

Tail	S_t/S	A	m	Normal fuselage; $l/b = 0.47$				Long fuselage; $l/b = 0.63$			
				C_{n_β}	$\Delta C_{n_{\beta_t}}$ Measured	$\Delta C_{n_{\beta_t}}$ Calculated	η_t	C_{n_β}	$\Delta C_{n_{\beta_t}}$ Measured	$\Delta C_{n_{\beta_t}}$ Calculated	η_t
				$T_c = -0.03$							
None	------	----	----	-0.034	-----	------	----	-0.050	------	------	----
1	0.090	1.00	1.50	.011	0.045	0.064	0.70	.006	0.056	0.086	0.65
2	.067	1.00	1.50	0	.034	.048	.72	-.007	.043	.064	.67
3	.090	2.28	2.50	.043	.077	.107	.72	.056	.106	.143	.74
4	.067	2.28	2.50	.027	.061	.080	.77	------	-----	-----	----
5	.090	2.28	2.50	------	-----	------	----	.092	.142	.143	1.00
				$T_c = 0.51$							
None	------	----	----	-0.062	-----	------	----	-0.111	------	------	----
1	0.090	1.00	1.50	------	-----	------	----	.024	0.135	0.199	0.68
3	.090	2.28	2.50	.125	0.187	0.249	0.75	.147	.258	.334	.77
5	.090	2.28	2.50	------	-----	-----	----	.018	.129	.143	.90

TABLE II

RATINGS OF LATERAL STABILITY AND CONTROL BASED ON PILOT'S OBSERVATIONS OF BEHAVIOR OF MODEL IN FLIGHT

Vertical tail	Flap deflection (deg)	Thrust coefficient, T_c	Normal fuselage				Long fuselage			
			Directional stability	Control			Directional stability	Control		
				Aileron and rudder	Aileron alone	Rudder alone		Aileron and rudder	Aileron alone	Rudder alone
1	0	-0.03	C	A-	B-	D	---	---	---	---
2			C	A-	C	---	C	A-	B-	D
3			B+	A	B+	C+	A	A	A-	C-
4			B-	A	B	---	B	A	A-	C-
1	0	.20	C+	A	B	D+	---	---	---	---
2			C	A-	C	---	---	---	---	---
3			A-	A	A-	---	A	A	A	D
4			B+	A	A-	---	B+	A-	A-	D+
1	60	-.03	B-	A	B+	D	---	---	---	---
2			C+	A	B+	---	---	---	---	---
3			A	A	A	C-	A	A	A	C
4			A-	A	A-	C	B+	A-	A-	D
1	60	.20	B	A	B+	D-	---	---	---	---
2			C+	A	B+	D	---	---	---	---
3			---	---	---	---	A	A	A	D
4			A-	A	A-	C	B+	A	A-	D

Rating	Stability	Control
A	Stable	Good
B	Slightly stable	Fair
C	Neutral	Poor
D	Unstable	Unsatisfactory

Figure 1.- Test section of NACA free-flight tunnel showing powered model in flight.

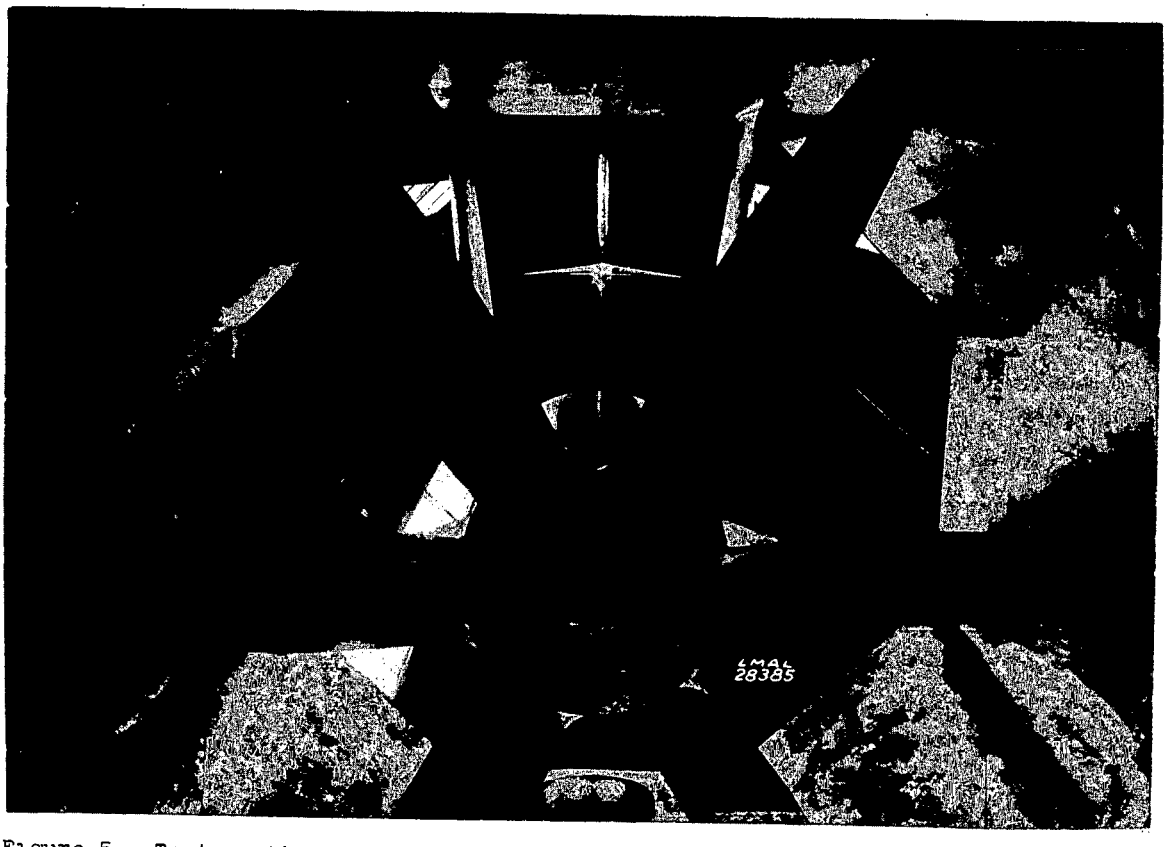

Figure 5.- Test section of NACA free-flight tunnel showing 1/10-scale model mounted on balance strut.

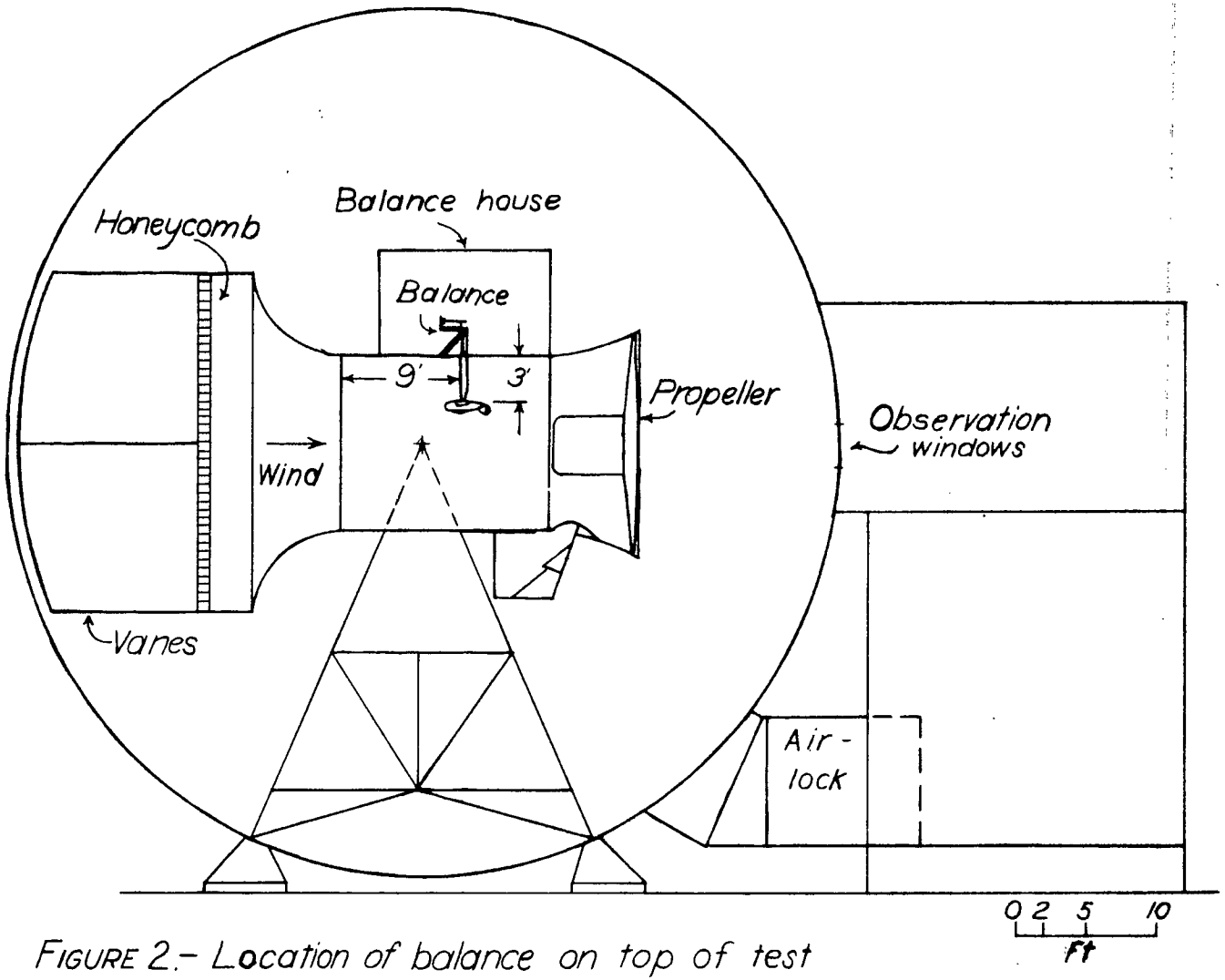

FIGURE 2.- Location of balance on top of test section of the free-flight tunnel.

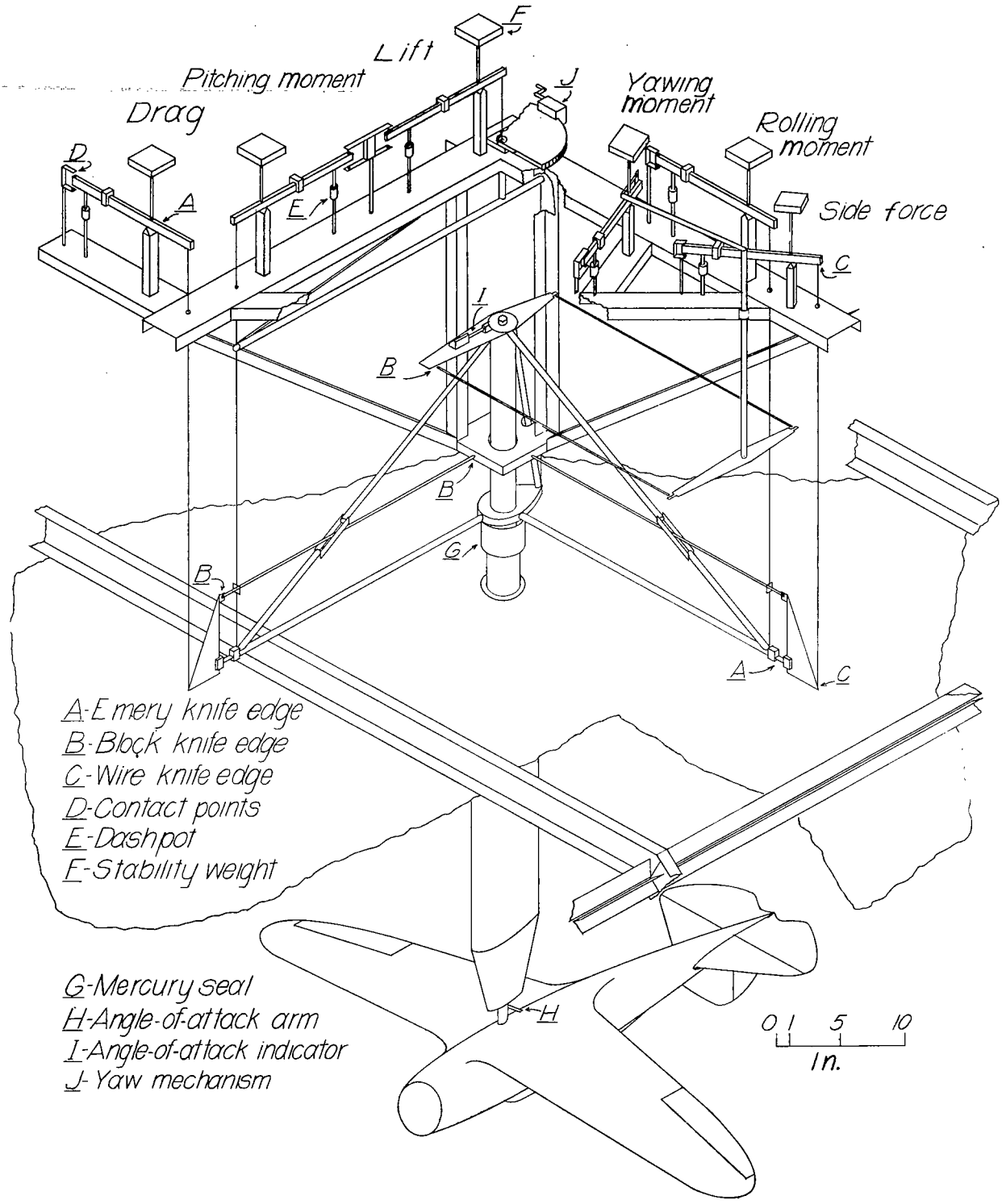

FIGURE 3.—Diagram of six-component balance in free-flight tunnel.

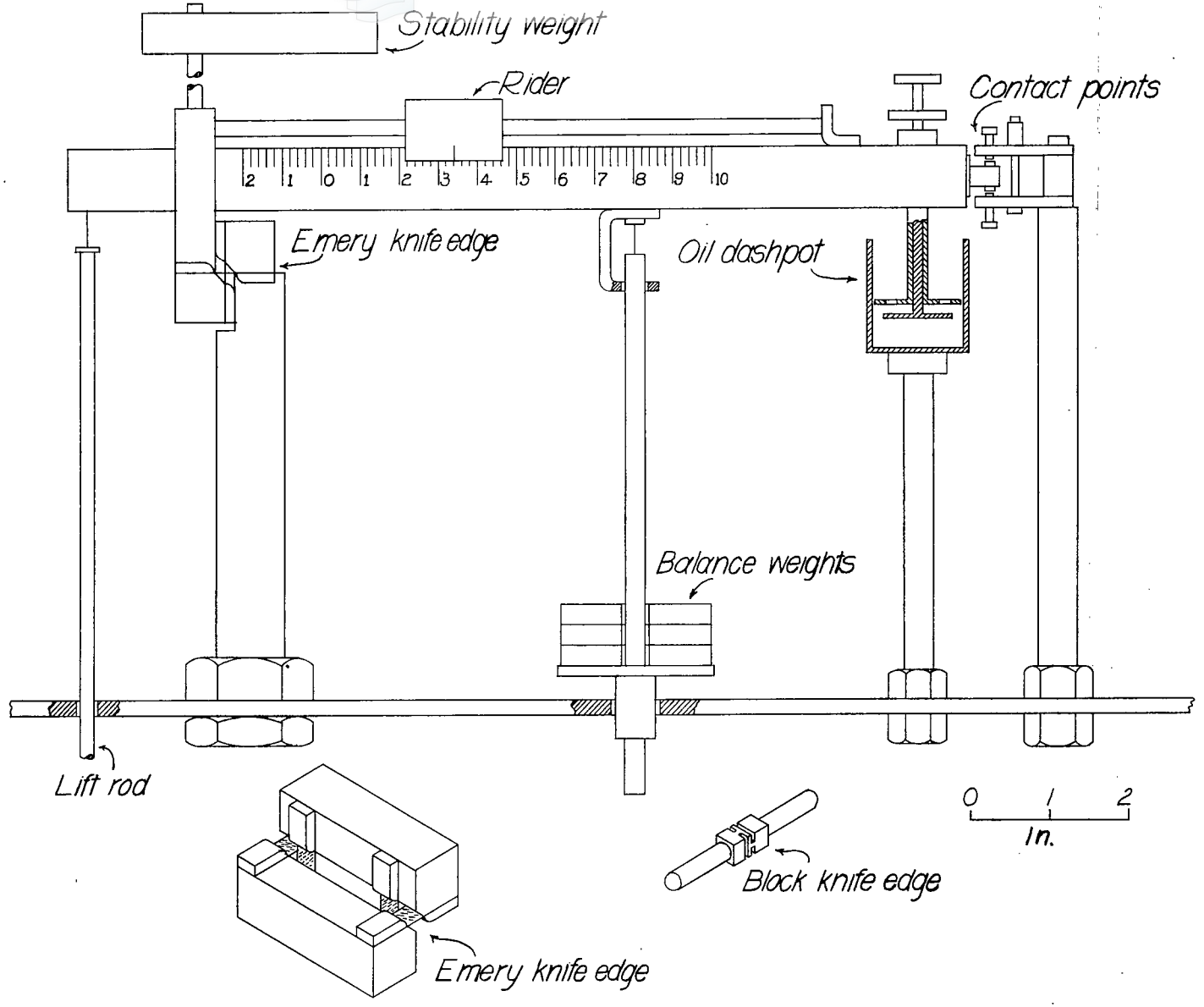

FIGURE 4.- Lift balance unit of free-flight-tunnel balance.

NACA

Fig. 6

Wing area = 2.237 sq ft
Average chord = 0.621 ft

(Use 1/80" scale)

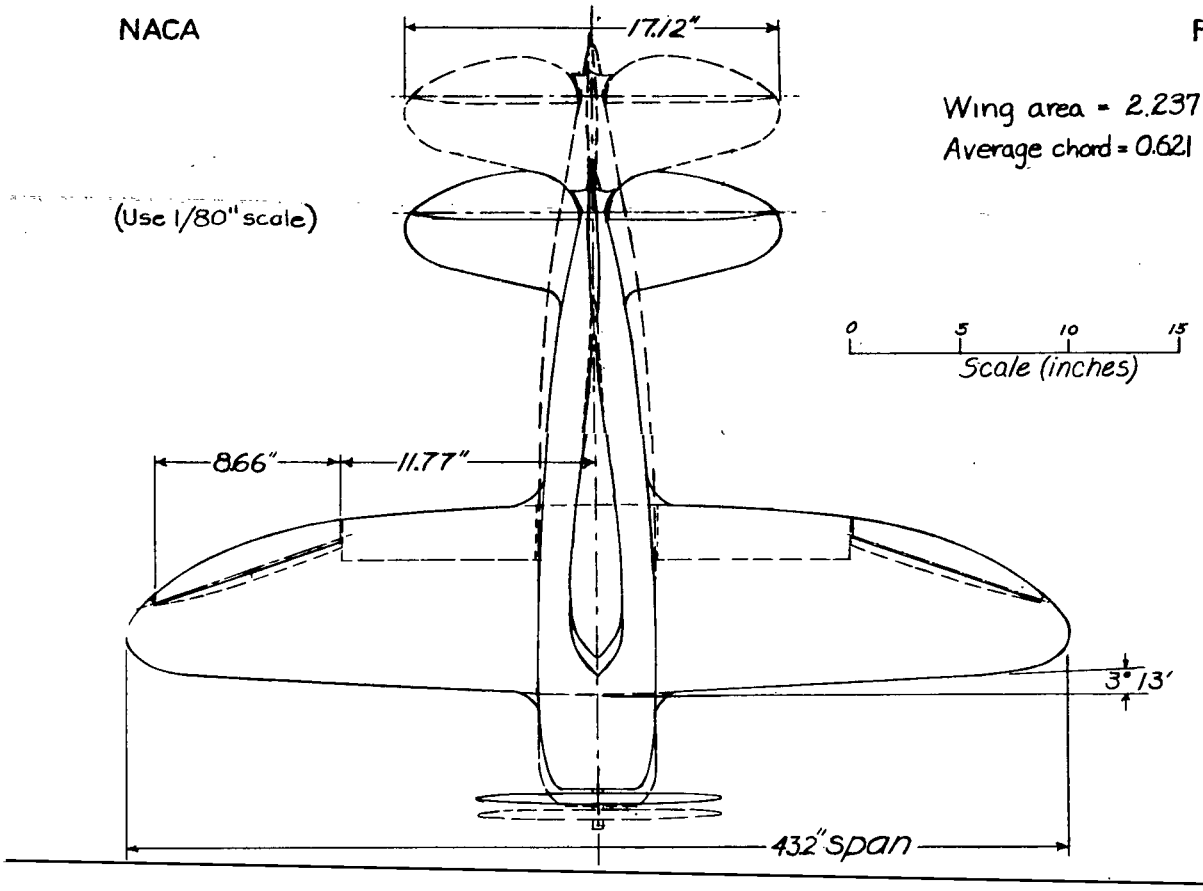

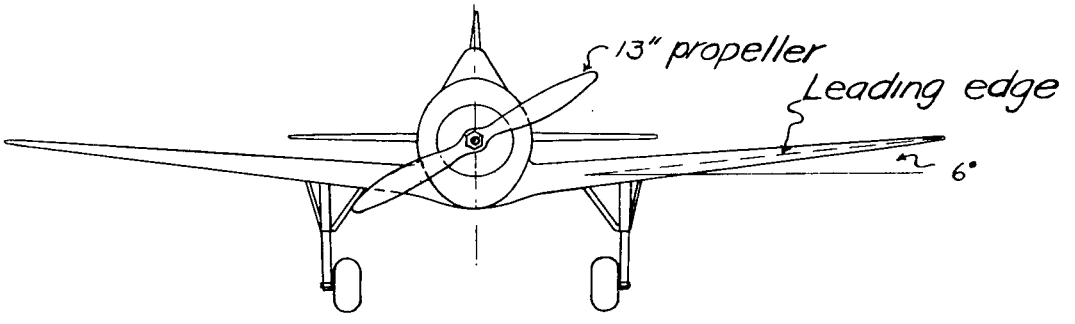

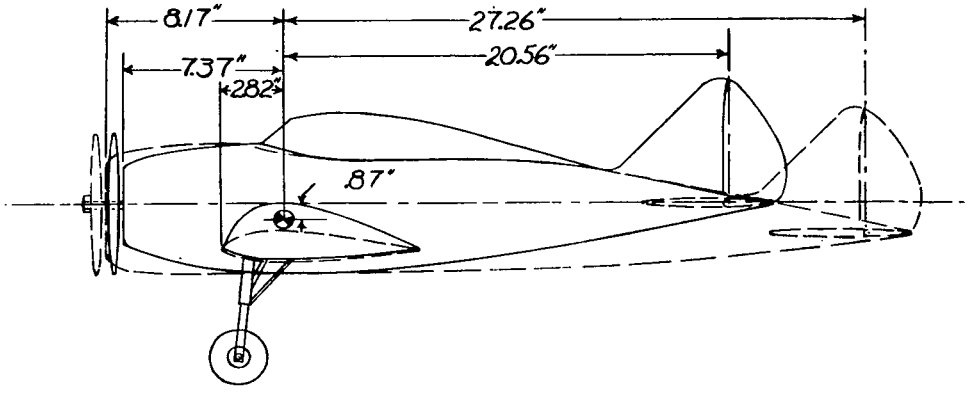

Figure 6.-The 1/10-scale powered model with normal and long fuselage as tested in the free-flight tunnel.

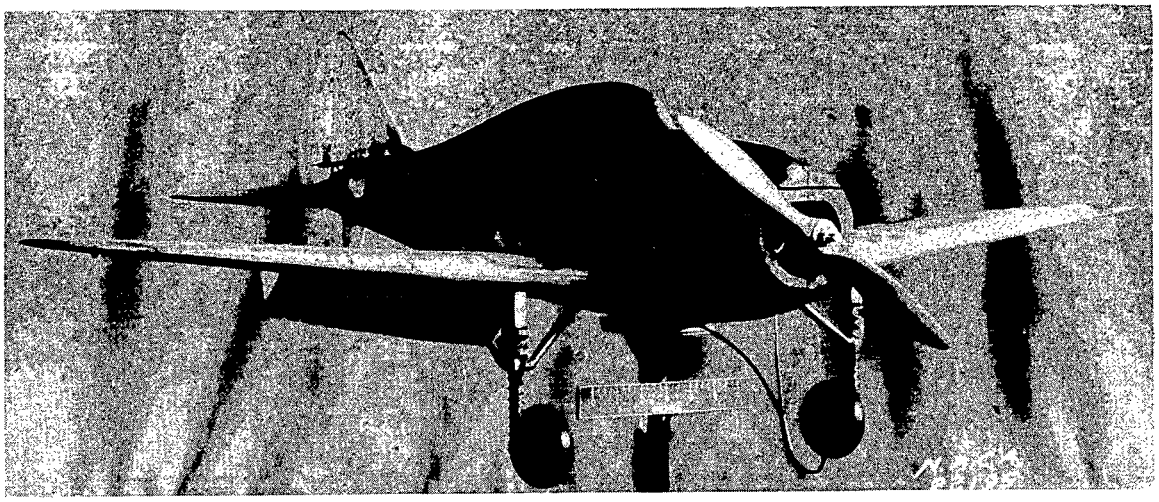

(a) Three-quarter ffont view.

Figure 7.- Views of 1/10-scale model with normal fuselage and tail 1.

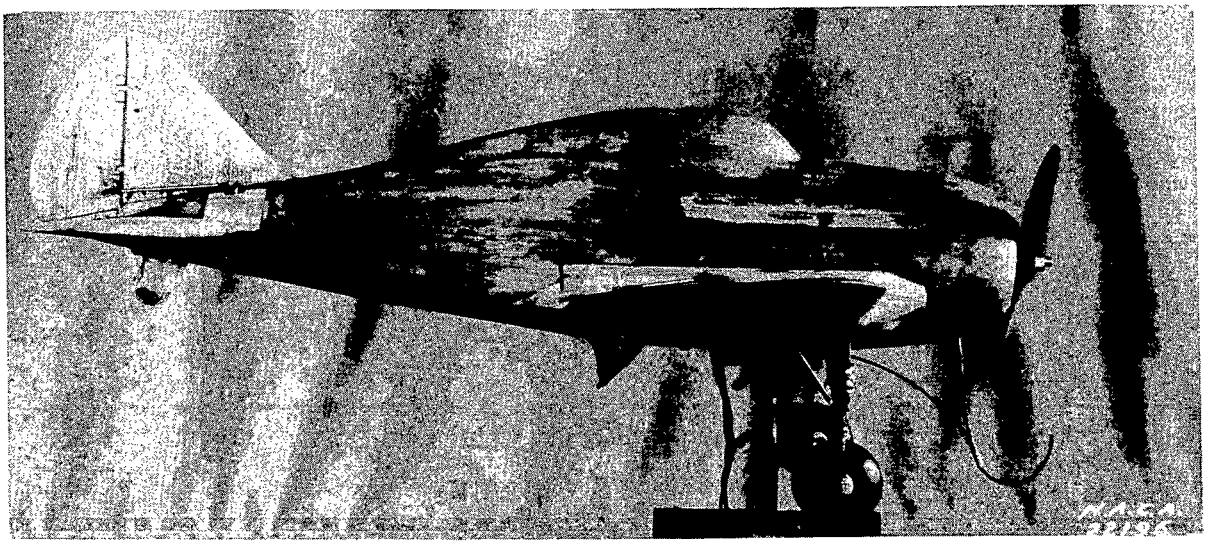

(b) Side view.

Figure 7.- Concluded.

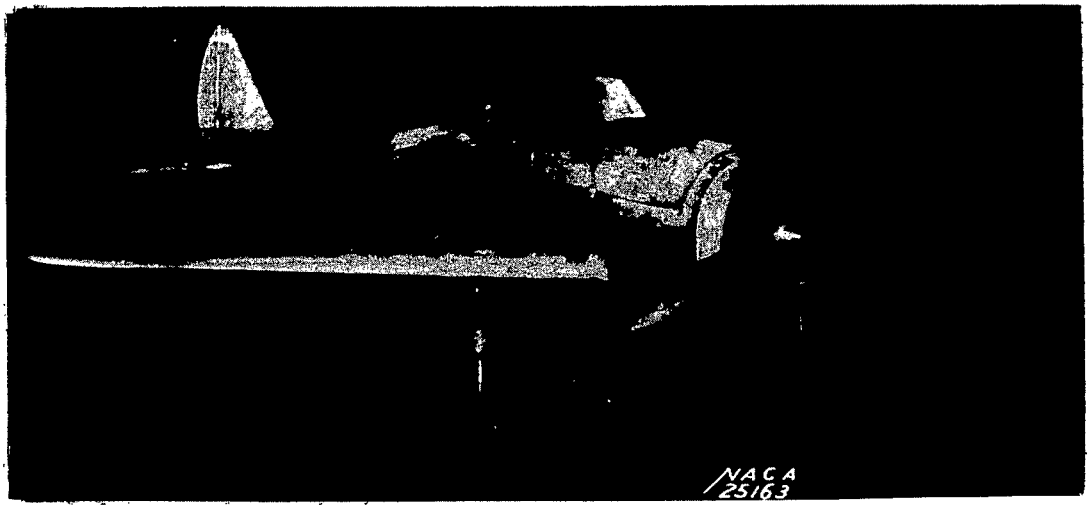

(a) Three-quarter front view.

Figure 8.- Views of 1/10-scale model with long fuselage and tail 2.

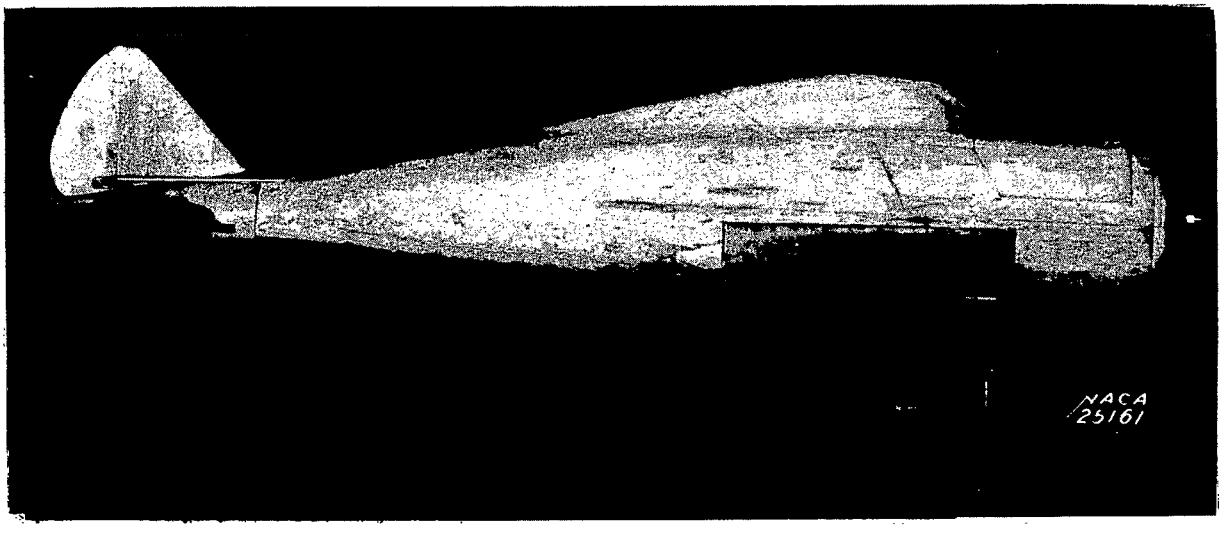

(b) Side view.

Figure 8.- Concluded.

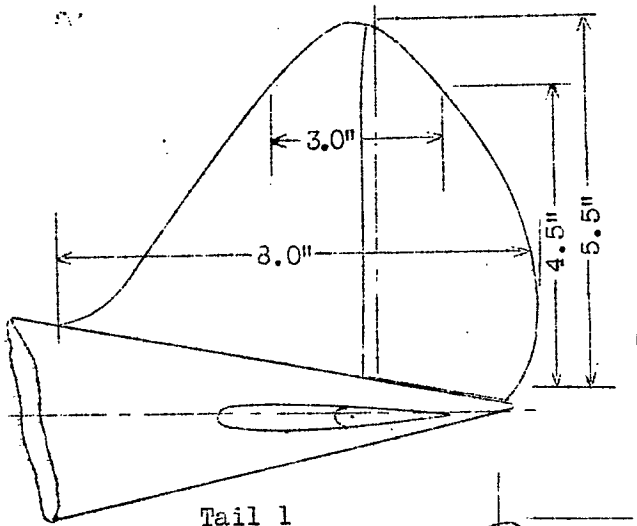

Tail 1

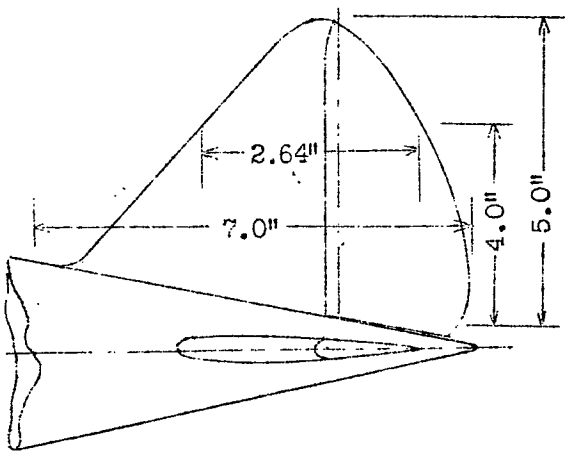

Tail 2

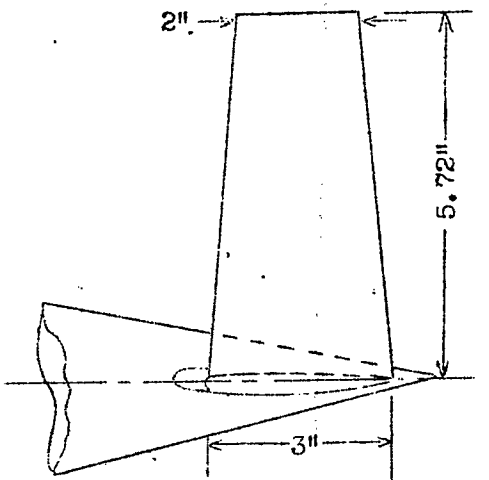

Tail 5 (twin tail)

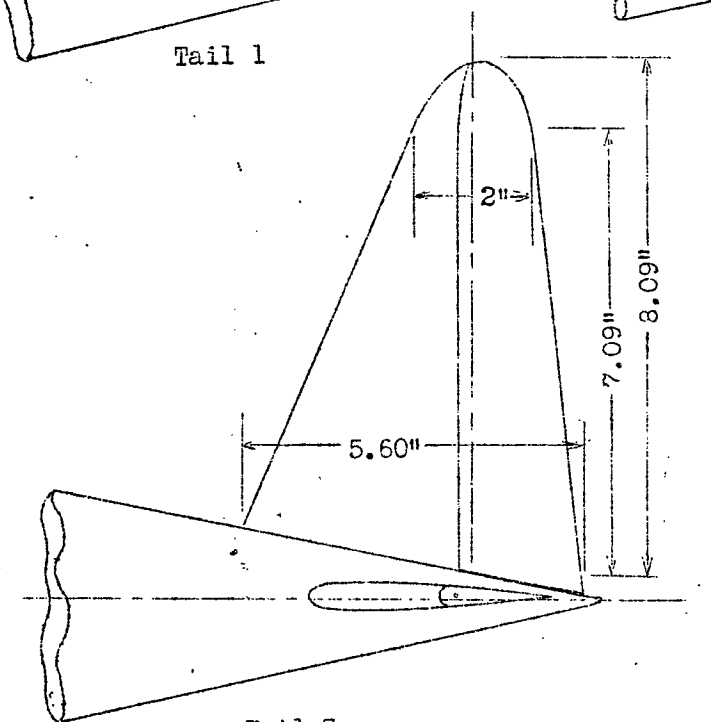

Tail 3

Figure 9.- Vertical tails used in tests of 1/10-scale model.

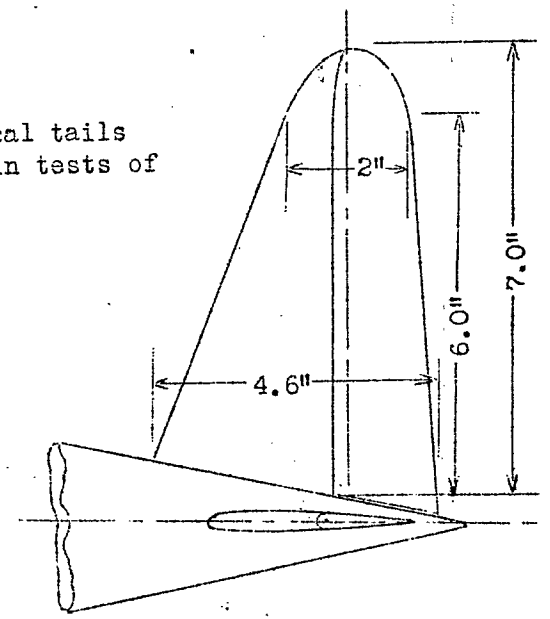

Tail 4

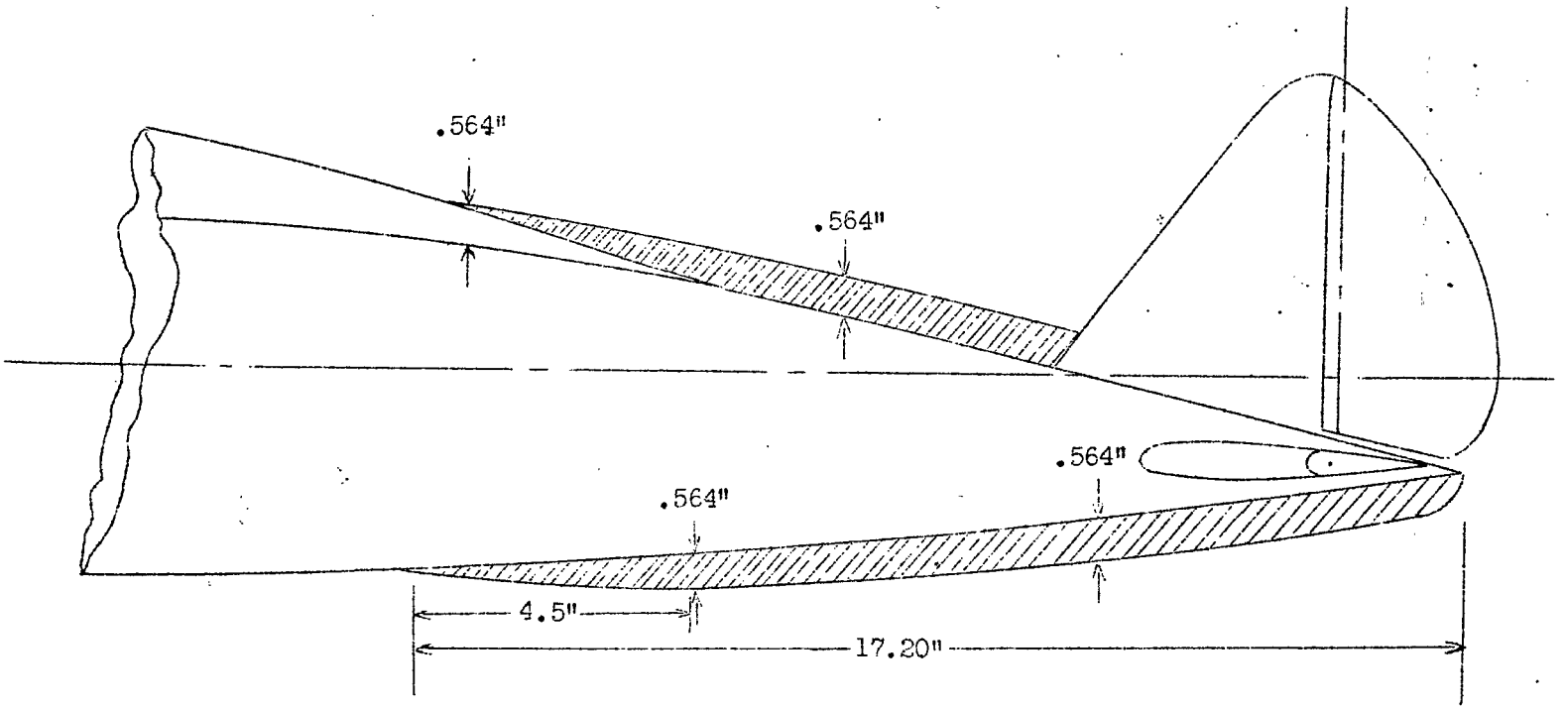

Figure 10.- Vertical tail (tail 1 + dorsal fin) as tested on model with long fuselage.

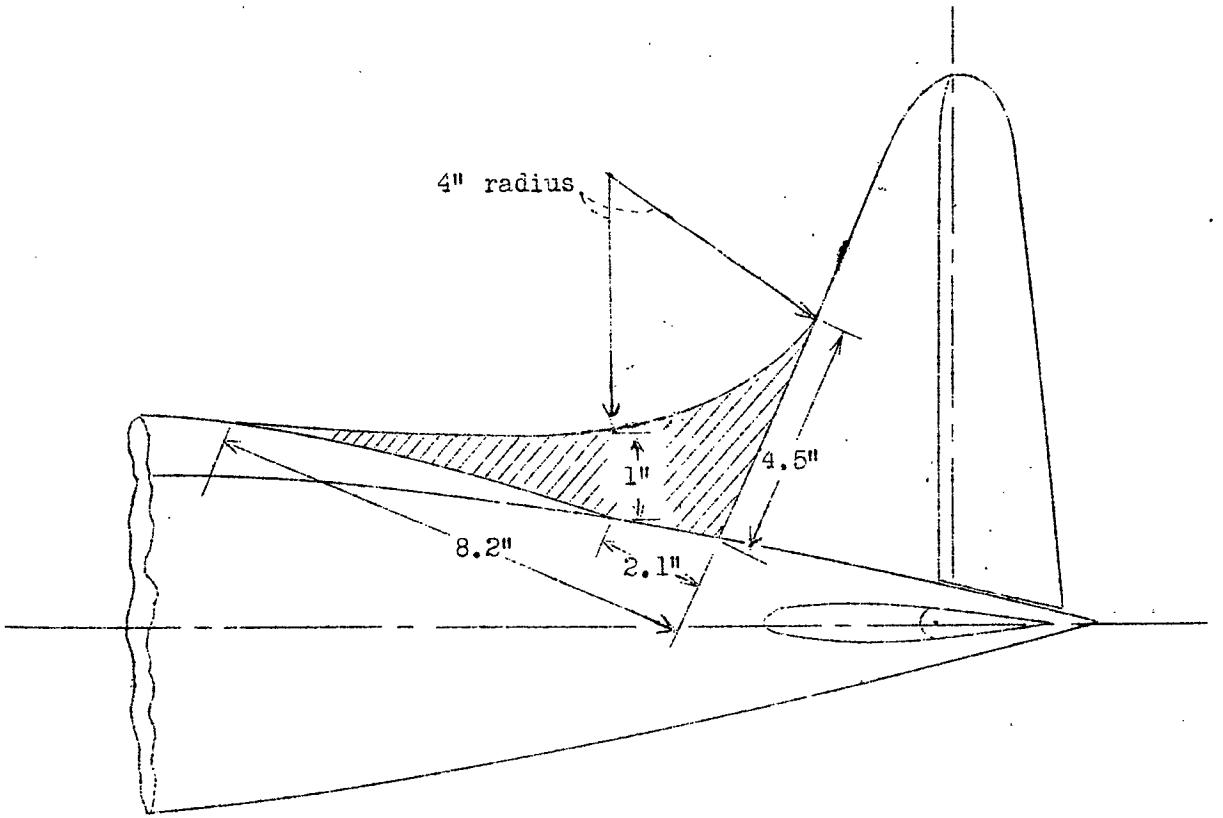

Figure 11.- Vertical tail (tail 3 + dorsal fin) as tested on model with normal fuselage.

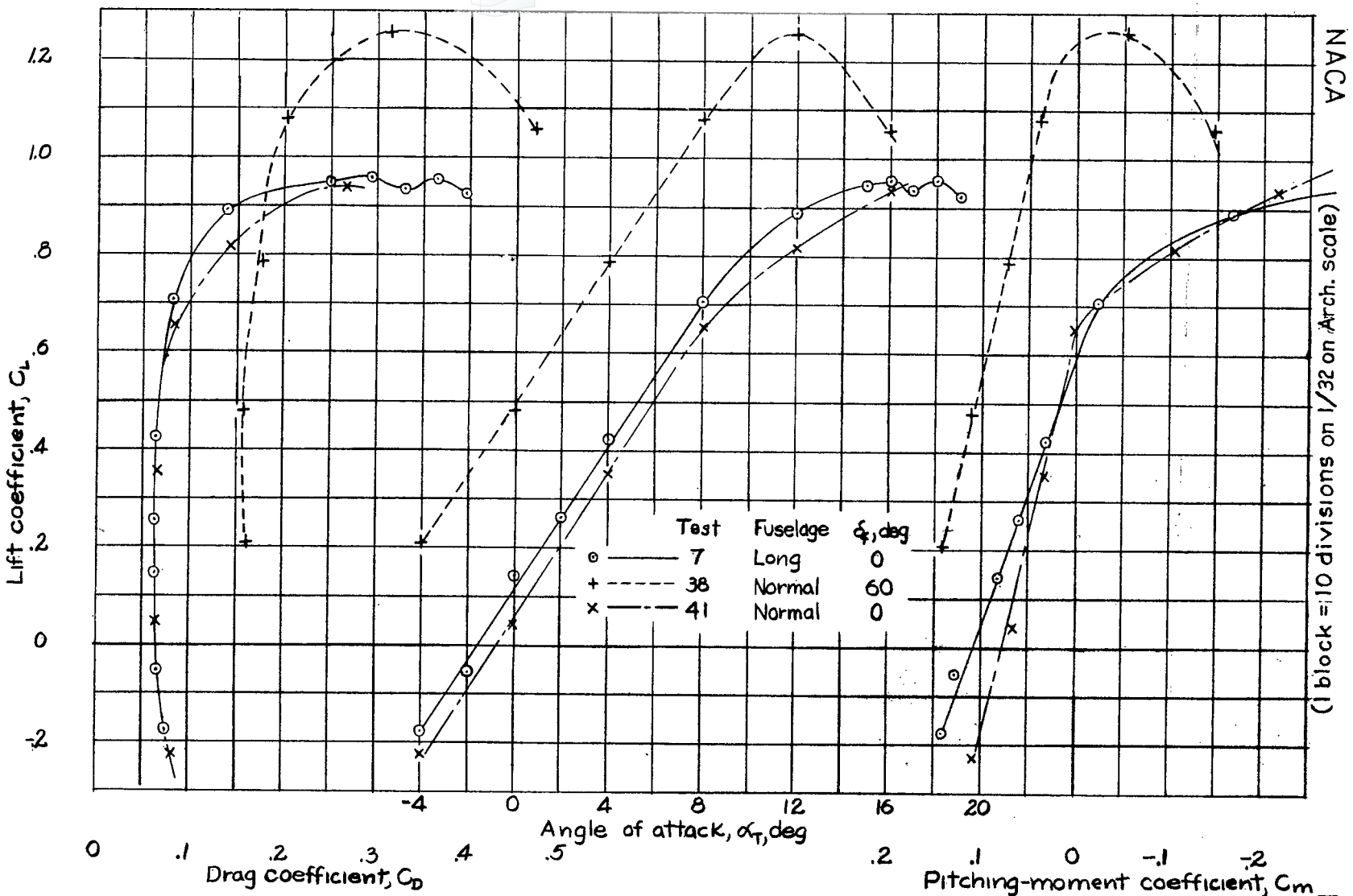

Fig. 12

FIGURE 12.- Lift, drag, and pitching-moment characteristics of the model without propeller.

NACA

Fig. 13

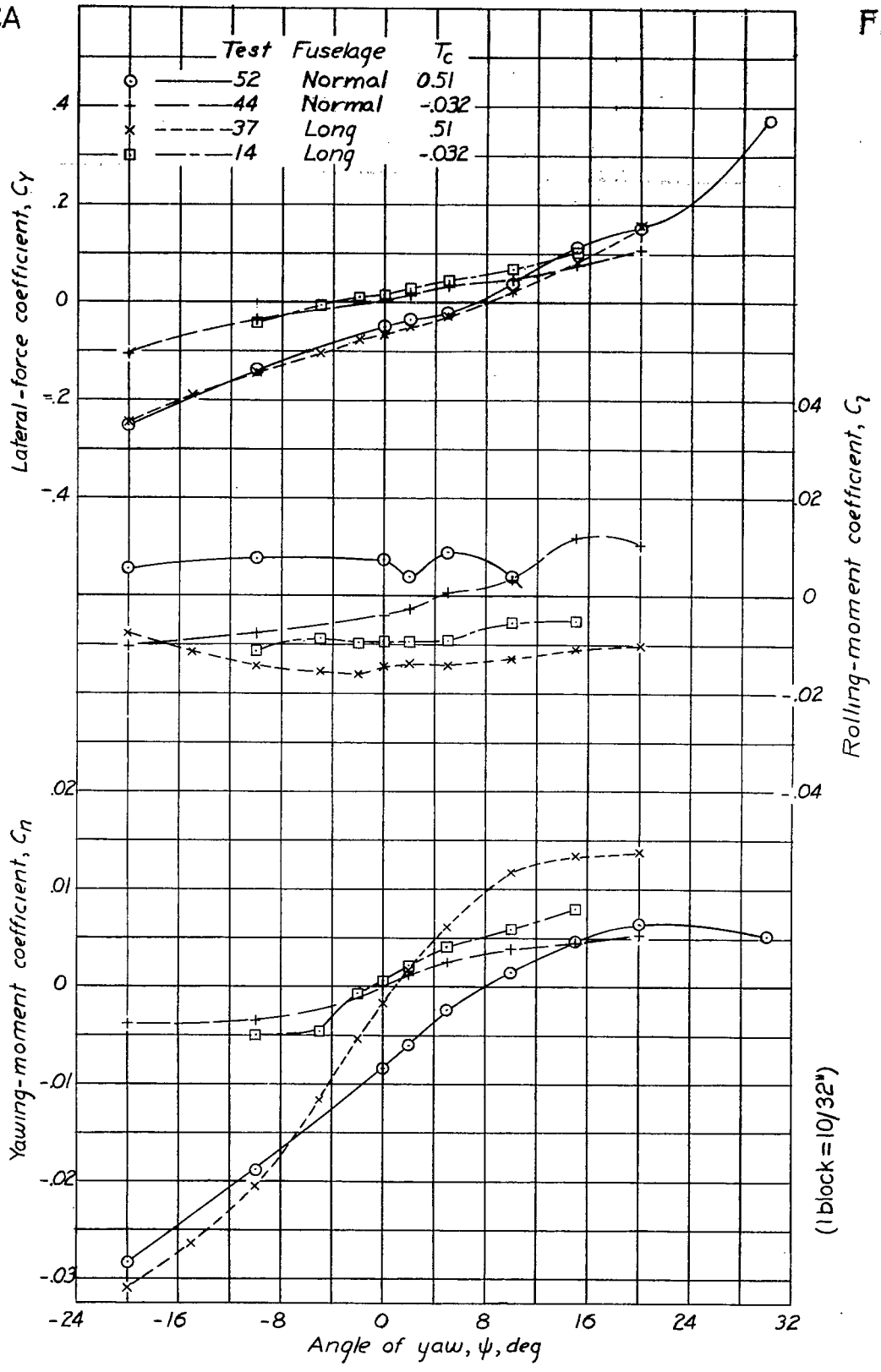

Figure 13.— The effect of fuselage length on the yaw characteristics of the model with the vertical tail off. $\alpha_T = 8°$; flaps neutral.

NACA

Fig. 14

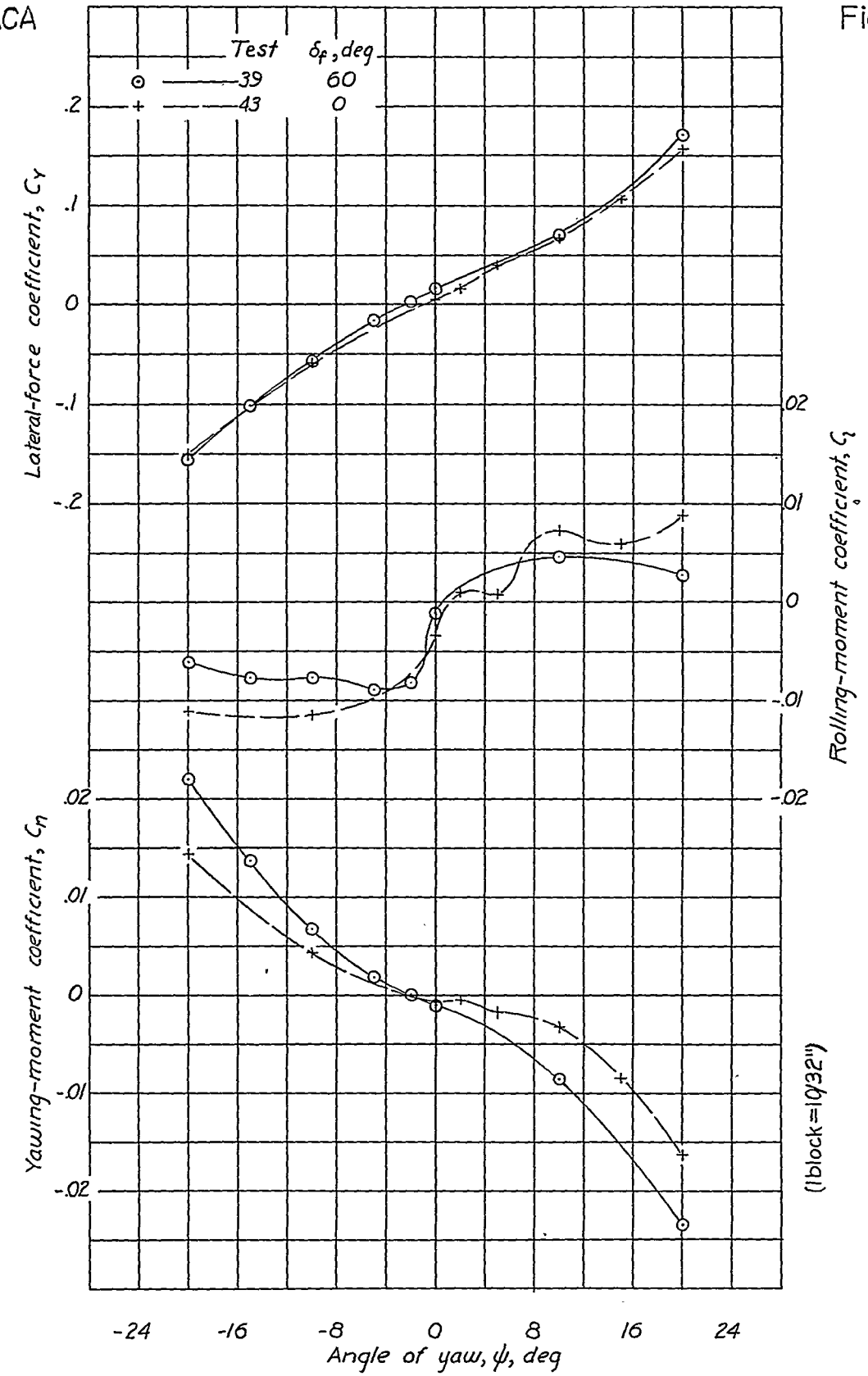

Figure 14.- The effect of flaps on the yaw characteristics of the model with normal fuselage and tail 1. $\alpha_T = 8°$; $T_C = -0.03$.

NACA

Fig. 15

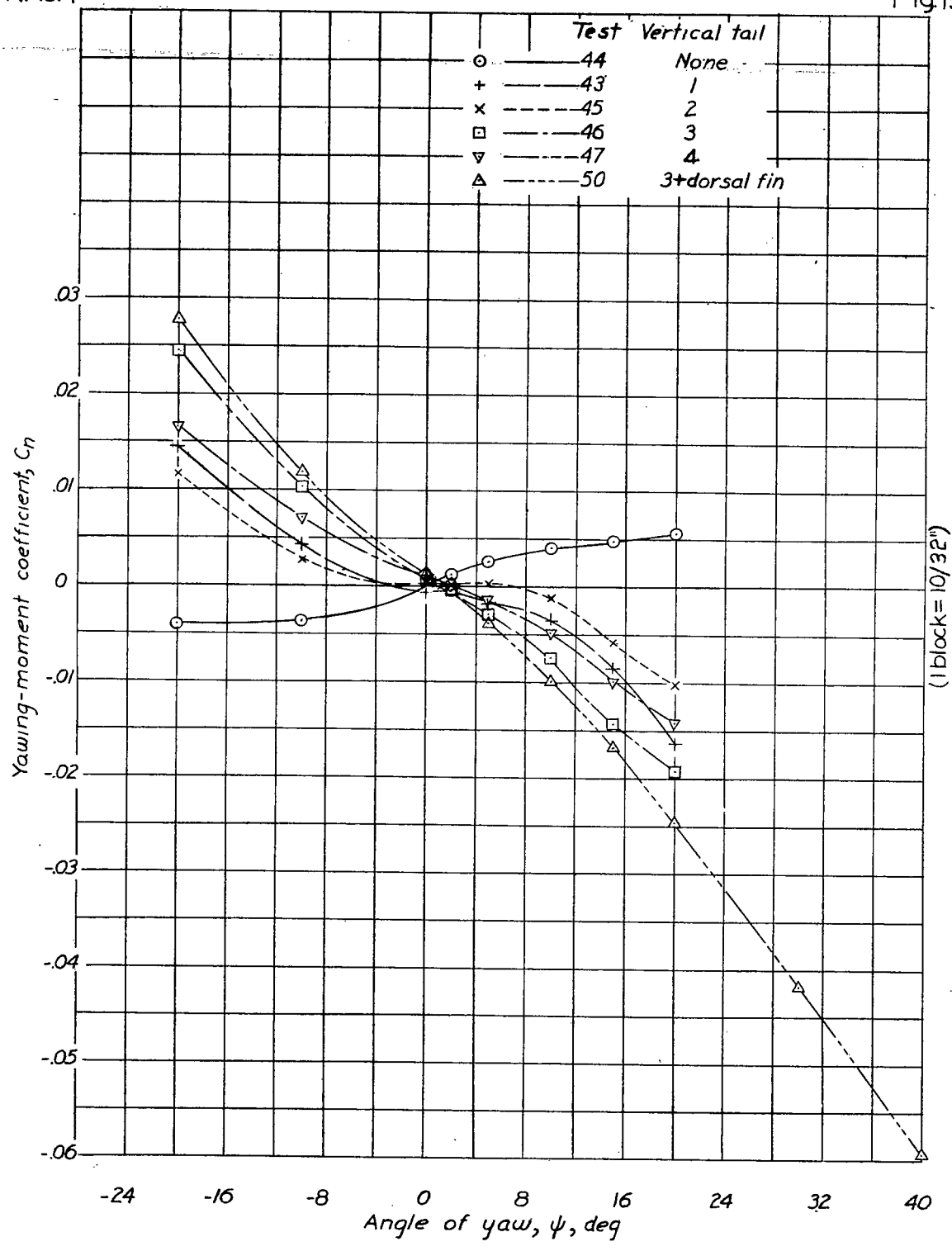

FIGURE 15.— The effect of vertical-tail arrangement on the yawing-moment due to yaw of the model with normal fuselage, with windmilling propeller. Flaps neutral; $\alpha_T = 8°$; $T_c = -0.03$.

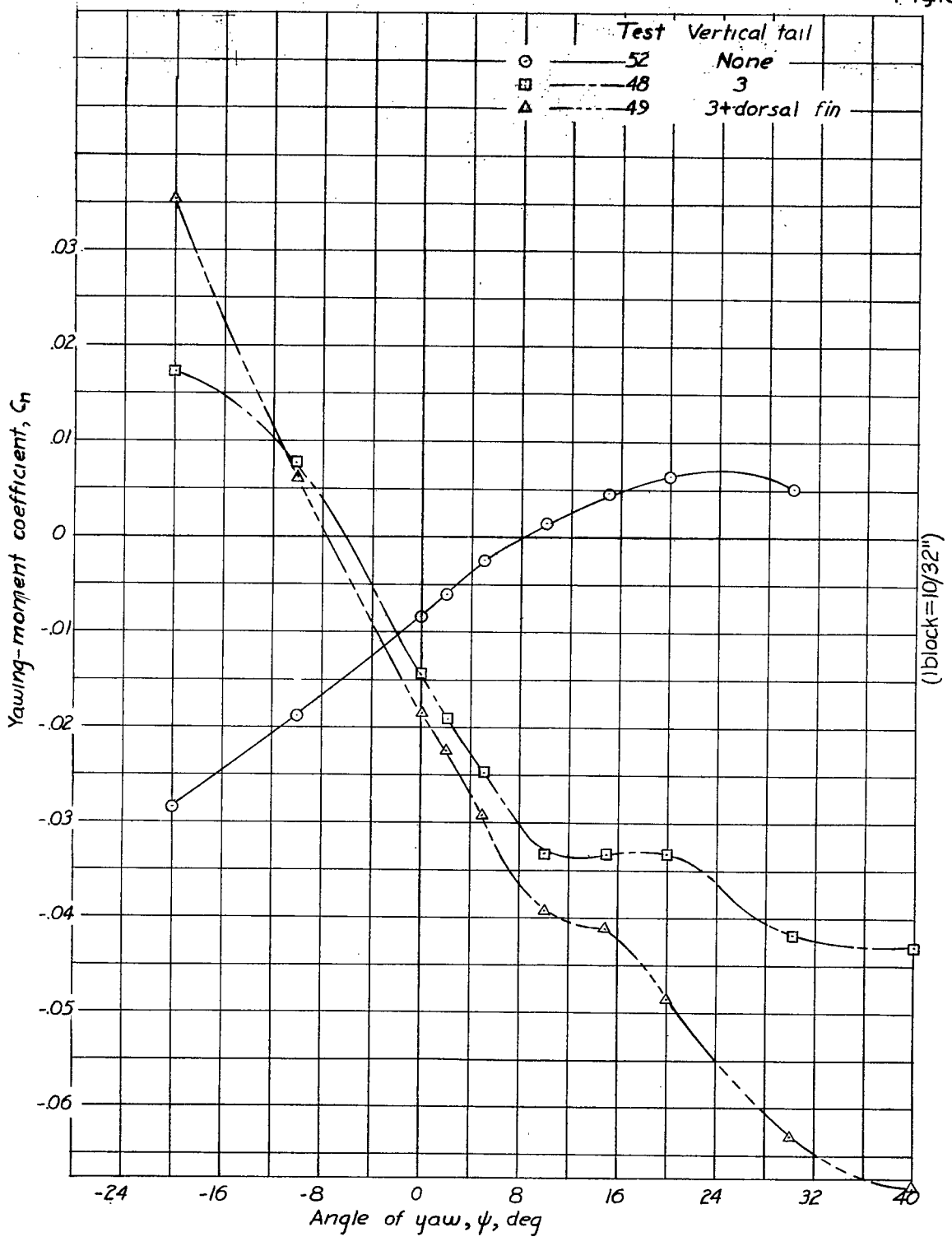

FIGURE 16.— The effect of vertical-tail arrangement on the yawing-moment due to yaw of the model with normal fuselage. Flaps neutral; $\alpha_T = 8°$; $T_c = 0.51$.

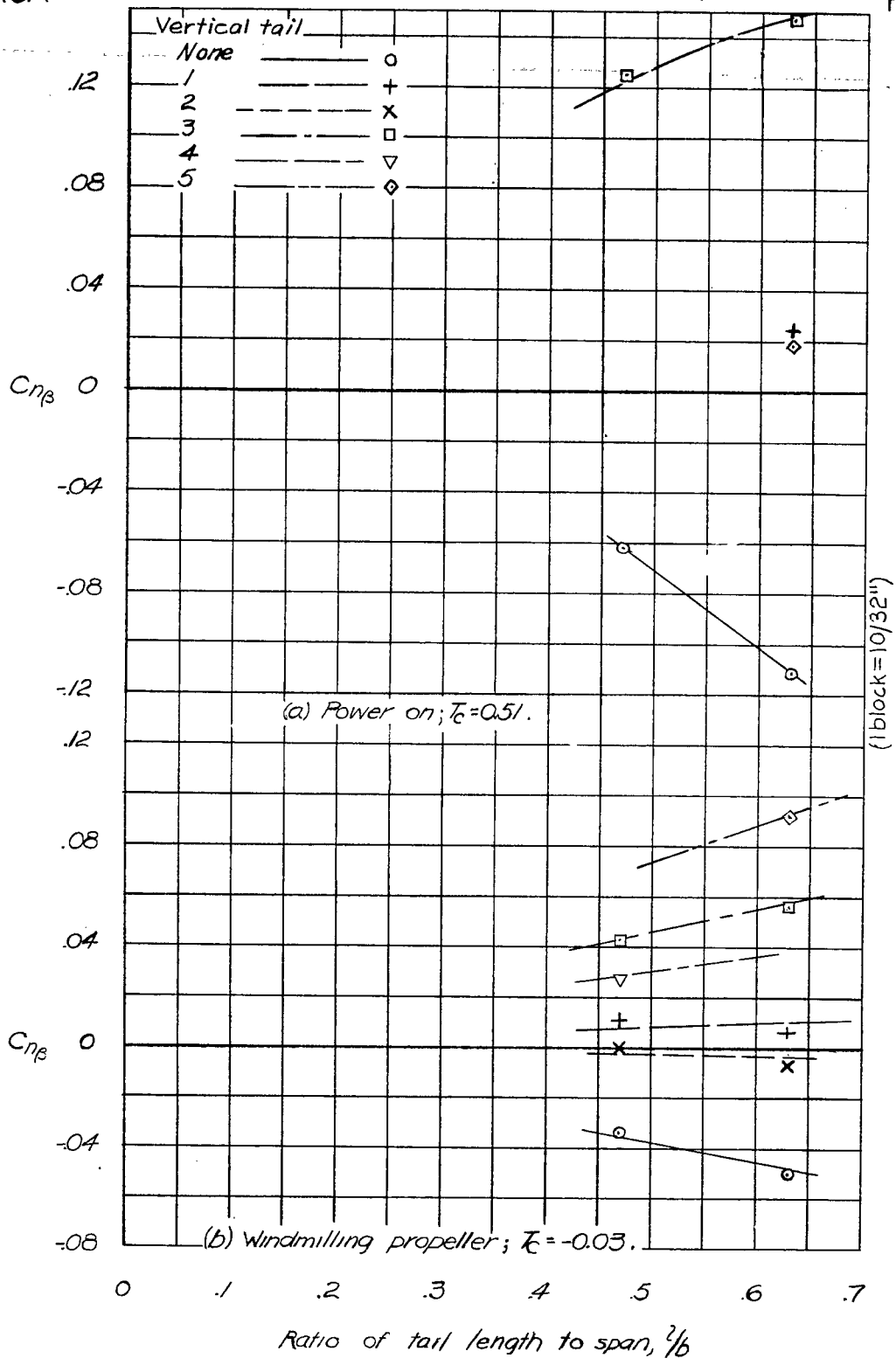

Figure 19.- Effect of fuselage length on directional-stability derivative C_{n_β} for various tails. Flaps neutral; $\alpha_T = 8°$.

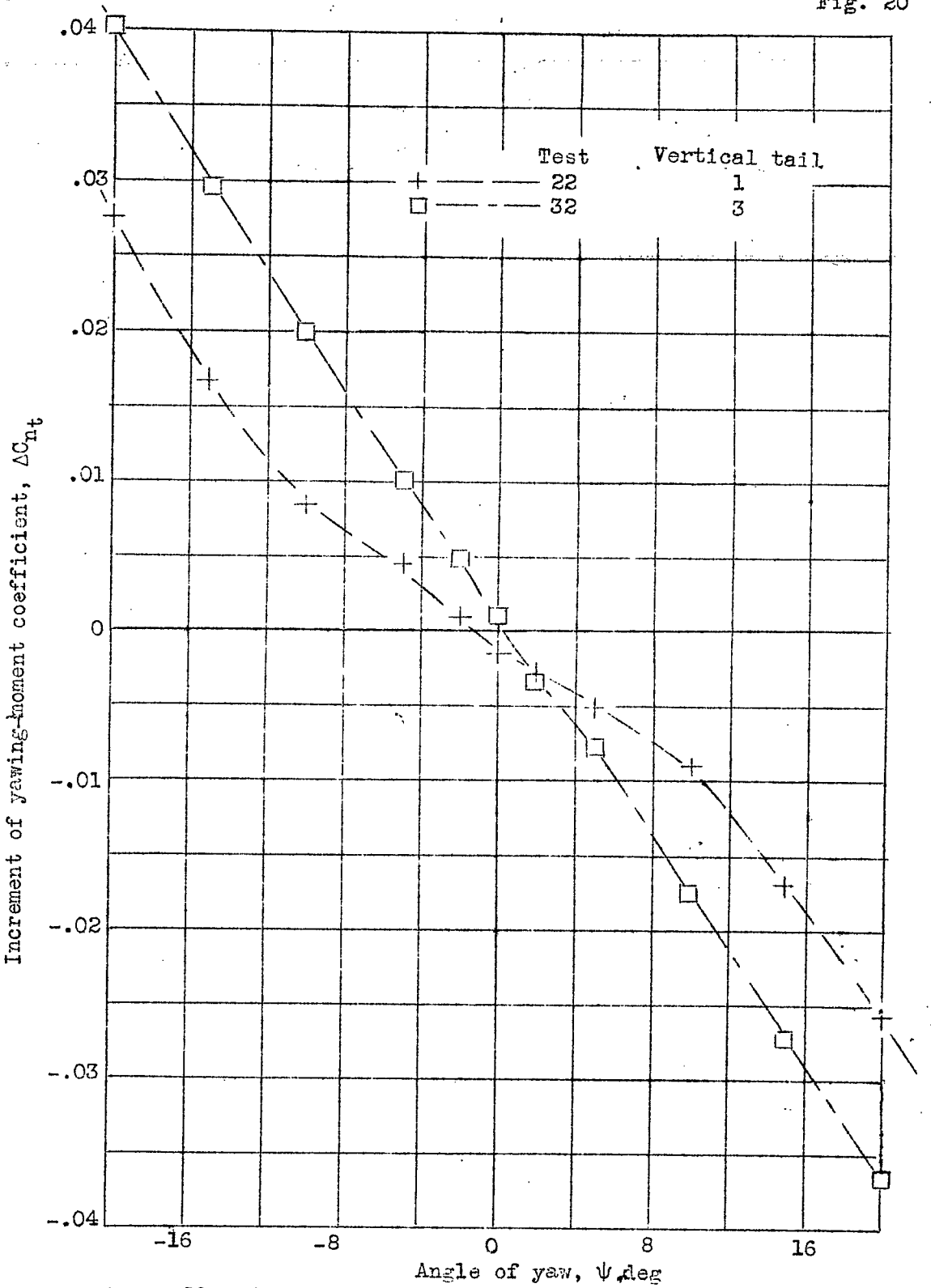

Figure 20.- Increment of yawing-moment coefficient due to vertical tail for the model with long fuselage. Propeller windmilling; $\alpha_T = 8^\circ$

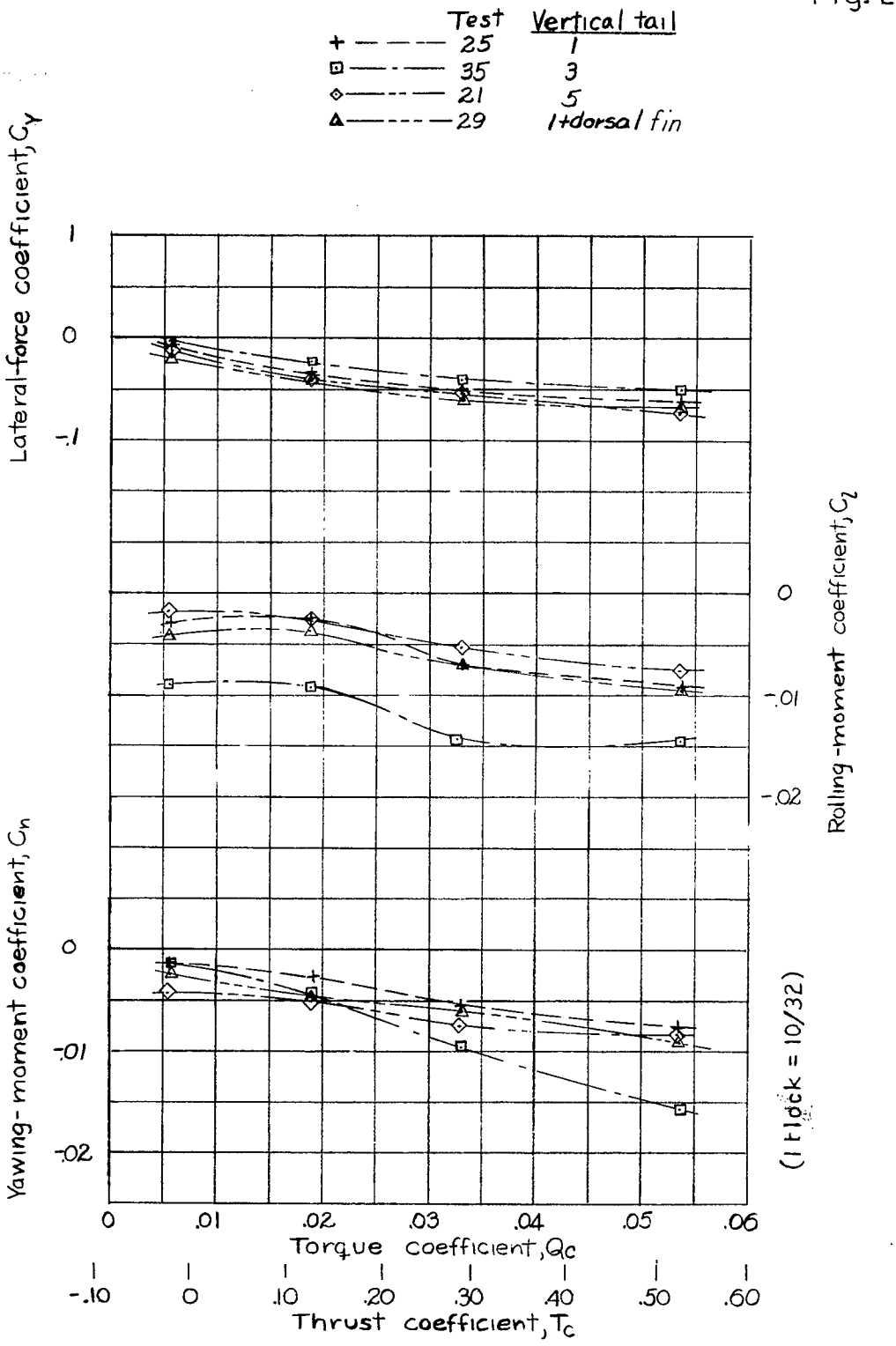

FIGURE 21.— Variation of rolling- and yawing-moment and lateral-force coefficients due to power for the model with long fuselage, flaps neutral, and various vertical-tail arrangements. $\alpha_T = 8°$; $\psi = 0°$.